HHS Public Access

Author manuscript

Neuroscience. Author manuscript; available in PMC 2022 March 01.

Published in final edited form as:

Neuroscience. 2021 March 01; 457: 74–87. doi:10.1016/j.neuroscience.2020.12.027.

The nAChR chaperone TMEM35a (NACHO) contributes to the development of hyperalgesia in mice

Sergey G Khasabov[1], **Victoria M Rogness**[1], **Montana B Beeson**[2], **Lucy Vulchanova-Hart**[3], **Li-Lian Yuan**[4], **Donald A Simone**[1], **Phu V Tran**[2,*]

[1]Department of Diagnostic and Biological Sciences, University of Minnesota, Minneapolis, Minnesota, USA

[2]Department of Pediatrics, University of Minnesota, Minneapolis, Minnesota, USA

[3]Department of Neuroscience, University of Minnesota, Minneapolis, Minnesota, USA

[4]Department of Physiology and Pharmacology, Des Moines University, Des Moines, Iowa, USA

Abstract

Pain is a major health problem, affecting over fifty million adults in the US alone, with significant economic cost in medical care and lost productivity. Despite evidence implicating nicotinic acetylcholine receptors (nAChRs) in pathological pain, their specific contribution to pain processing in the spinal cord remains unclear given their presence in both neuronal and non-neuronal cell types. Here we investigated if loss of neuronal-specific TMEM35a (NACHO), a novel chaperone for functional expression of the homomeric α7 and assembly of the heteromeric α3, α4, and α6-containing nAChRs, modulates pain in mice. Mice with *tmem35a* deletion exhibited thermal hyperalgesia and mechanical allodynia. Intrathecal administration of nicotine and the α7-specific agonist, PHA543613, produced analgesic responses to noxious heat and mechanical stimuli in *tmem35a* KO mice, respectively, suggesting residual expression of these receptors or off-target effects. Since NACHO is expressed only in neurons, these findings indicate that neuronal α7 nAChR in the spinal cord contributes to heat nociception. To further determine the molecular basis underlying the pain phenotype, we analyzed the spinal cord transcriptome. Compared to WT control, the spinal cord of *tmem35a* KO mice exhibited 72 differentially-expressed genes (DEGs). These DEGs were mapped onto functional gene networks using the knowledge-based database, Ingenuity Pathway Analysis, and suggests increased neuroinflammation as a potential contributing factor for the hyperalgesia in *tmem35a* KO mice. Collectively, these findings implicate a heightened inflammatory response in the absence of

*Corresponding Author: Phu V Tran, MMC 391 Mayo, 420 Delaware St, SE, Minneapolis, MN 55455, USA, tranx271@umn.edu, Ph: 612-626-7964.

Author contributions: Conceptualization, S.G.K., D.A.S. and P.V.T; Data curation, S.G.K., V.M.R, M.M.B and P.V.T; Formal analysis, S.G.K and P.V.T; Funding acquisition, D.A.S and P.V.T; Investigation, S.G.K and P.V.T; Methodology, S.G.K and P.V.T; Project administration, P.V.T; Resources, M.M.B, L.V-H, L-L.Y, D.A.S and P.V.T; Supervision, P.V.T; Writing – original draft, P.V.T, Writing – review & editing, S.G.K, D.A.S and P.V.T.

Disclosures: All authors have no conflicts of interest to declare.

neuronal NACHO activity. Additional studies are needed to determine the precise mechanism by which NACHO in the spinal cord modulates pain.

Keywords

Pain; TMEM35a/NACHO; spinal transcriptome; nicotinic acetylcholine receptor; inflammation

Introduction

The International Association for the Study of Pain estimated that 20% of adults worldwide suffer from chronic pain and almost 10% of the population is diagnosed with pain every year. This makes pain a major health problem costing society an estimated $560 billion annually in medical care and lost productivity in the US (Dahlhamer et al. 2018; Gaskin and Richard 2012). These statistics, in addition to the ongoing opioid epidemic, underscore the need to develop new and effective treatments to manage persistent pain.

Nicotinic acetylcholine receptors (nAChR) are ligand-gated cationic channels assembled as homo- or heteropentamers from α- (α2–10) and β- (β2–4) subunits (Crespi et al. 2017; Kabbani and Nichols 2018). The roles nAChRs in modulating pain remain unclear. Nicotine produced analgesia in experimental models of chronic pain (Aceto et al. 1986; Christensen and Smith 1990) and this was blocked by the non-selective nAChR antagonist, mecamylamine (Freitas et al. 2015; Saika et al. 2015). Antinociceptive effects of nicotine and its derivatives were associated with a decrease in sensitization of spinal neurons (Holtman et al. 2010). In clinical studies, nicotine patches decreased pain evoked by cutaneous electrical stimulation (Jamner et al. 1998), intranasal nicotine decreased postoperative pain (Flood and Daniel 2004; Matthews et al. 2016), and nicotine deprivation increased neurogenic inflammation and mechanical hyperalgesia in daily tobacco smokers (Ditre et al. 2018), suggesting analgesic effects of nicotine in humans. However, the selective α4β2 receptors agonist, ABT-894, was ineffective in a clinical trial for diabetic neuropathic pain (Rowbotham et al. 2012). The disparate effects of drugs targeting nAChRs between preclinical models and humans are well known, especially in the treatment of neuropathologies and psychiatric disorders (Bertrand and Terry 2018). Thus, the roles of specific nAChRs in pain require additional investigation. (+/−)-Epibatidine, a non-selective α7, α4β2, and α3β4 receptor agonist, reduced heat and mechanical hyperalgesia in models of inflammatory and neuropathic pain (AlSharari et al. 2012; Gao et al. 2010; Kesingland et al. 2000; Nirogi et al. 2013; Sullivan et al. 1994). Intrathecal epibatidine potentiated the analgesic effect of clonidine, an agonist for the α2-adrenergic receptor, in the formalin model (Hama et al. 2001). Epibatidine given directly into the rostral ventromedial medulla reduced hyperalgesia following inflammation, suggesting a role for α7, α4β2, and α3β4 in descending pathways that modulate nociception (Jareczek et al. 2017). As such, the role of each receptor subtype in the spinal cord in pain modulation remains unclear. Activation of the α7 receptor by selective agonists reduced inflammatory and neuropathic pain (Feuerbach et al. 2009; Loram et al. 2012; Medhurst et al. 2008; Munro et al. 2012; Umana et al. 2017). The attenuation of inflammatory pain produced by the α7 nAChR agonist compound B was blocked by intrathecal application of an α7 nAChR antagonist (Medhurst et al. 2008).

However, α7 receptor knockout mice showed little changes in thermal and mechanical sensitivity at baseline or following nerve injury, whereas mice with a single copy of α7 gain-of-function, such as the L250T mutant mouse (Orr-Urtreger et al. 2000) characterized by increased α7 receptor affinity for agonists, exhibited decreased thermal hyperalgesia following nerve injury (Alsharari et al. 2013). Wieskopf et al. (2015) demonstrated a key role of the spinal α6-containing receptor, but not α4, in the modulation of mechanical allodynia in rodent models of inflammatory and neuropathic pain utilizing gene knockout and gain-of-function transgenic mice (Wieskopf et al. 2015). On the other hand, intrathecal α-conotoxin MII, a selective α6β2 and α3β2 receptor antagonist with a greater affinity for α6-containing receptors (>1000x), reduced baseline mechanical sensitivity in rats, implicating these receptors in the modulation of pain at the spinal cord level (Young et al. 2008).

In addition to the role of specific nAChRs in pain modulation, the mechanisms by which nAChRs modulate pain are unclear. Possibilities include inhibition of glutamate release from primary afferent nociceptive fibers (Young et al. 2008), or through nAChR-dependent activation of GABAergic neurons in the spinal cord, thereby enhancing inhibitory tone (Enna and McCarson 2006; Rashid et al. 2006; Umana et al. 2013). Indeed, there is evidence that activation of nAChR increased GABA release in the spinal cord (Genzen and McGehee 2005; Gonzalez-Islas et al. 2016). Activation of GABAergic neurons inhibited synaptic transmission, resulting in decreased pain signaling, whereas blocking GABA receptors produced hyperalgesia (Hwang and Yaksh 1997). Decreased GABAergic inhibition has been implicated in the development of neuropathic pain (Larsson and Broman 2011). Yet another possible mechanism by which nAChRs modulate pain is the suppression of neuroinflammation in the spinal cord through activation of nAChRs expressed on microglia. Activation of α4β2 or α7 nAChR by perineural or intrathecal administration of selective receptor agonists (e.g., TC-2559, PHA-543613, choline) decreased neuropathic pain, and this was associated with decreased microglial activity and release of pro-inflammatory mediators (Ji et al. 2019; Kiguchi et al. 2018; Loram et al. 2010). Given the presence of nAChRs in both neuronal and non-neuronal cell types, the roles of nAChRs in specific cells (e.g., neurons, microglia) and the specific contributions of nAChR subtypes to pain modulation need further study.

Transmembrane protein 35a (TMEM35a) is a small neuronal-specific transmembrane protein (Kennedy et al. 2016; Tran et al. 2010), which has been renamed Novel Acetylcholine receptor Chaperone (NACHO) (Gu et al. 2016). NACHO was demonstrated to be necessary and sufficient for assembly and trafficking the homomeric α7 while facilitates the assembly of the heteromeric α3, α4, and α6 containing receptor subtypes (Deshpande et al. 2020; Gu et al. 2016; Matta et al. 2017; Mazzaferro et al. 2020). Deletion of the *tmem35a* gene, which removes NACHO (polypeptide) activity, resulted in a complete absence of α7 membrane expression and electrophysiological activity (Gu et al. 2016). However, *tmem35a* KO mice showed residual cell surface expression of α3, α4- and α6-containing receptors evident by residual binding of epibatidine and conotoxin II (Gu et al. 2016; Matta et al. 2017; Mazzaferro et al. 2020). We took advantage of *tmem3a* KO mice to determine the effect of NACHO (and α7) on evoked pain. We found that *tmem35a* KO mice exhibited thermal hyperalgesia and mechanical allodynia accompanied by an increased number of microglia in the spinal cord dorsal horn. Due to the complete loss of α7 nAChR functional activity, we further determined the precise role of neuronal α7 in the *tmem35a* KO mice via intrathecal administration of the selective α7 receptor agonist, PHA543613. Our findings support a role for α7 nAChR in modulating activity of sensory neurons evoked by noxious heat.

Materials and Methods

Animals

Male *tmem35a* knockout (KO) mice (C57BL6/N) were bred in our lab on a C57Bl6/J background and maintained as previously described (Kennedy et al. 2016). C57Bl6/J (WT) littermates served as controls. Mice had access to food and water *ad libitum* and maintained on a 12 hr:12 hr (light: dark) cycle. Genotypes were determined using tail DNA and PCR amplification as previously described (Kennedy et al. 2016). The University of Minnesota Institutional Animal Care and Use Committee approved all protocols in this study.

Sensitivity to mechanical stimuli

Mechanical paw withdrawal threshold was used to determine differences in sensitivity to mechanical stimuli between *tmem35a* KO mice (n=20) and WT mice (n=18). The 50% mechanical threshold (g) was determined using the up-down method (Chaplan et al. 1994) with an adjustment for mouse paw sensitivity (Hamamoto et al. 2007). Briefly, mice were placed on a wire mesh platform, covered with a glass container (10×3.5×3.5cm) and allowed to acclimate to the environment for at least 30 min before each of 3 daily test sessions. A series of 8 calibrated von Frey monofilaments (0.07, 0.16, 0.40, 0.60, 1.0, 1.2, 2.0, and 4.0 g) was used and stimuli were applied to the plantar surface of each hind paw. Testing was initiated with a monofilament that delivered 0.60 g. In the absence of a withdrawal response, a stronger monofilament was applied. If a withdrawal occurred, a weaker monofilament was presented. The inter-stimulus interval was ~5 sec. The resulting pattern was tabulated, and the 50% paw withdrawal threshold was calculated. The 50% mechanical paw withdrawal threshold was determined for each hind paw. Paw withdrawal threshold for each mouse was defined as the mean threshold of both paws. Mechanical allodynia was defined as a significant decrease in mean paw withdrawal threshold compared to WT mice or vehicle treatment.

Sensitivity to heat stimuli

Heat sensitivity was assessed using methods previously described (Khasabov et al. 2017). Briefly, radiant heat was applied to the plantar surface of each hind paw and withdrawal response latencies were determined. Before testing, mice were placed under a clear plastic cage (10×3.5×3.5 cm) on a clear, 3-mm thick glass elevated to allow maneuvering of a controlled radiant heat source underneath. Mice (15 WT and 16 KO) were acclimated to the testing chamber daily for 15 min before testing on 3 consecutive days. Heat stimuli of constant intensity were delivered by a 50-W light bulb placed in a custom case, which allowed focusing the light source (8-mm diameter) on the plantar surface of one hind paw. The intensity of the lamp was adjusted to produce stable withdrawal latencies ~ 7–13 s in control mice. Withdrawal latencies were measured to the nearest 0.1 s using a photocell that terminated the trial and a timer upon a withdrawal response. Each hind paw received four stimuli, alternating between each hind paw, with a minimum of 1 min between trials. Withdrawal latency for each hind paw was defined as the mean of the last three trials, and withdrawal latencies for each paw were averaged. A 19-s cutoff was imposed on the stimulus duration to prevent tissue damage. Heat hyperalgesia was defined as a significant decrease in mean withdrawal response latency as compared to WT mice or vehicle treatment.

Sensitivity to cold stimuli

A cold plate apparatus (Ugo Basile, Gemonio, Italy) was used to compare cold sensitivity between KO (n=12) and WT (n=10) mice. Mice were individually habituated in the apparatus with the plate temperature set at 30˚C. Following 30 min habituation, the plate temperature was adjusted to 4˚C. Sensitivity to cold was measured as the number of nocifensive behaviors (paw lifts, bouts of licking, and jumps) that occurred during a 3-min test session. Cold hyperalgesia was defined as an increase in the number of nocifensive behaviors (paw lifting and licking and jumping) as compared to WT mice or vehicle treatment.

Drugs

All compounds were diluted with saline (0.9% NaCl). (−) Nicotine bitartrate was purchased from Sigma (St. Louis, MO) and PHA543613 hydrochloride was purchased from Tocris (Biotechne, Minneapolis, MN).

Intrathecal drug administration and experimental design

Mice were randomly divided into separate groups and drugs were administered by intrathecal (i.t.) injection according to the previously described method (Hylden and Wilcox 1980). Briefly, mice were handled for 2 days prior to injection to acclimate them to the handling procedure for the injection. Each mouse was held firmly by the pelvic girdle and injection was performed with a disposable (30-gauge, ½ inch) needle attached to a 50 μl Hamilton syringe. The needle was inserted on one side of L5 or L6 spinous processes at an angle 20° to horizontal plane. It was placed between the spinous and transvers processes and reached the intrathecal space at the level of cauda equine to avoid damage to the spinal cord. The needle was placed at 10° and the tip moved rostrally approximately 0.5 cm, and 5μl of the drug solution was delivered. Successful placement of the needle was indicated by a tail flick reflex. The needle was removed immediately after injection. Separate groups of mice received nicotine at doses of 0.5 or 1.5 nmol, or PHA543613 at doses of 10 or 50 nM. Sensitivity to mechanical, heat, and cold stimuli was determined as described above and was determined just prior to i.t. injection and at 15, 30, 60, and 90 min after injection. Sample sizes were 4–10/genotype/treatment. The experimenter was blinded to the treatment.

Immunohistochemistry and Imaging

Mice (n=4/genotype) were transcardially perfused with cold PBS and 4% Paraformaldehyde fixative. L4-L6 spinal cord were embedded in OCT compound (Scigen Scientific, Gardena, CA) and cryo-sectioned at 20 μm and mounted onto Superfrost Plus glass slides. Sections were rehydrated in PBS, permeabilized in 0.1% Triton X-100 (in PBS), blocked in 10% BSA (Fraction V, Sigma), and incubated in primary antibodies overnight at 4°C. Sections were rinsed (3X) with PBS + 0.1% Tween-20 (PBST), blocked in 10% BSA, and incubate in fluorescent conjugated secondary antibodies overnight at 4°C. Excess antibodies were removed with PBST rinses (3X). Sections were clear with aqueous mounting media containing DAPI (Vector laboratories Inc.) and covered with a glass coverslip. Confocal images were captured with a Nikon Digital-Eclipse C1 system equipped with a motorized stage. Primary antibodies included Biotinylated-Isolectin B_4 (IB4, 1:500, Vector laboratories Inc.), rabbit polyclonal anti-NACHO (1:100, In-house antibody, (Kennedy et al. 2016)), mouse monoclonal anti-CGRP (1:1000, Santa Cruz Biotechnology Inc., Santa Cruz, CA), rabbit polyclonal anti-Iba1 (1:1000, Novus Biologicals), and CF488-conjugated α-bungarotoxin (1:50, Biotum). Secondary antibody (purchased from Vector Laboratories Inc.) included Alexa-488 anti-rabbit IgG (1:200), Alexa-555 anti-rabbit IgG (1:200), Alexa-633 anti-mouse IgG (1:200), and Alexa-555 Avidin (1:200). Images of spinal cords were captured by a laser confocal microscope (Nikon Eclipse C1) or an upright microscope equipped with a CCD camera (Leica DM6B system). Confocal images were captured using 10x or 20x air objectives with adjusted laser power to optimize signal-to-noise ratio and minimize signal saturation. Pseudocolors (red, green, and blue) were assigned to the three channels to produce optimal contrast signals. Images were processed using Adobe Photoshop (v21.1.0).

Quantitation of microglia in the dorsal horn

Cells immunoreactive for ionized calcium binding adaptor molecule 1 (Iba1), a specific marker for microglia/macrophage, were estimated by counting $Iba1^+$ cells across representative sections (n=3 sections per mouse). Iba1 labeled cells were counted in lamina I through III of the dorsal horn from 5 WT and 4 KO mice. The experimenter counting the cells was blinded to the mouse genotype.

Spinal cord transcriptome and bioinformatics

Spinal cords (T8-L6) were isolated from adult mice (n=4/genotype) for RNA isolation (RNAqueous, Invitrogen). RNA sequencing (RNAseq) was performed as previously described (Barks et al. 2018). Briefly, isolated RNA was quantified using the RiboGreen RNA Assay kit (Invitrogen) and assessed for quality using capillary electrophoresis (Agilent BioAnalyzer 2100; Agilent). RNA samples with RIN value ≥ 8.0 were used for library construction. Barcoded libraries were constructed for each sample using the TruSeq RNA v2 kit (Illumina). Libraries were size (200 bp) selected and sequenced (50 bp paired-end reads) using Illumina HiSeq 2500. Quality control on raw sequence data was performed with FastQC. Mapping of reads was performed via Hisat2 (version 2.1.0) using the mouse genome (mm10) as reference. Differentially-expressed genes (DEGs) were identified by genewise negative binomial generalized linear models using the EdgeR feature in CLC Genomics Workbench (Qiagen, version 10.1.1). The generated list was filtered based on false discovery rate (FDR) corrected *p*-value (*q*-value) < 0.05. DEGs were annotated by Ingenuity pathway Analysis (IPA; Qiagen) to identify relevant altered canonical pathways, molecular networks and cellular functions. Statistical significance ($p < 0.05$) was determined by Fisher's exact test.

Statistical methods

Mechanical withdrawal thresholds, heat withdrawal latencies and the number of nocifensive behaviors evoked by cold were compared between WT and KO mice using t-tests. Effects of i.t. administration of nicotine and PHA543613 were compared over time between KO and WT mice using 2-way ANOVA with repeated measures (dose and time as independent factors). Post hoc comparisons were made using Bonferroni's multiple comparisons test. Unpaired t-test was used for Iba^+ cell counting to determine the difference between WT and KO mice. For transcriptomic analysis, EdgeR statistical package was used for determining differentially expressed genes with and FDR (q value) < 0.05. For IPA analysis, Fisher's exact test was used for multiple comparisons to determine significant gene interactions, canonical pathways, and molecular networks. Where applicable, graphs and statistical analyses were generated using Prism Graphpad 8 (Graphpad Software, San Diego, CA). For all statistical tests, a p value <0.05 was considered significant. All data are expressed as mean ± SEM.

Results

Expression of NACHO in spinal cord

Expression of NACHO (TMEM35a) was visualized by immunostaining using a polyclonal antibody raised against the C-terminal 15-amino acids of NACHO (Kennedy et al. 2016). NACHO immunostaining was found in the spinal cord dorsal horn of WT (Fig. 1A) but not in the *tmem35a* KO mice (Fig. 1B). There were no differences in localization within dorsal horn architecture between WT and KO mice based on the immunostaining of calcitonin gene-related peptide (CGRP) fibers in lamina I and Isolectin B_4 (IB4) fibers in lamina II (Fig. 1C–D). NACHO was co-localized with peptidergic fibers marked with CGRP in dorsal horn lamina I (Fig. 1C), with much less co-localization with non-peptidergic fibers that were labeled with IB4 in lamina II (Fig. 1D). NACHO expression was found in cells that also expressed cell surface α7 nAChR marked by α-bungarotoxin binding ($\alpha Bgtx^+$) in lamina I, II, V, and VI (Fig. 1E–F).

tmem35a KO mice exhibited hyperalgesia compared to WT mice

Given the antinociceptive roles of nAChRs in various pain models (Freitas et al. 2015; Kesingland et al. 2000; Rowley et al. 2008), we assessed whether *tmem35a* KO mice exhibited mechanical allodynia and thermal hyperalgesia. Compared to WT littermates, KO mice exhibited lower mechanical withdrawal response thresholds (Fig. 2A), lower withdrawal latencies to heat (Fig. 2B) and increased number of nocifensive behaviors to cold (Fig. 2C). Mean mechanical response thresholds for WT and KO were 1.00 ± 0.09 and 0.15 ± 0.02 g, respectively ($t = 9.55$, $df = 36$, $p < 0.0001$). Mean withdrawal latencies to heat were 8.64 ± 0.40 sec for WT and 5.77 ± 0.24 sec for KO mice ($t = 6.28$, $df = 29$, $p < 0.0001$), and the mean numbers of nocifensive responses (paw lifting and licking and jumping) to cold were 2.6 ± 0.6 for WT and 12.4 ± 1.93 for KO mice ($t = 4.29$, $df = 19$, $p < 0.0004$).

Analgesia produced by intrathecal administration of nicotine is reduced in tmem35a KO mice

To determine if the loss of nAChR function is responsible for the hyperalgesia in *tmem35a* KO mice, mechanical withdrawal thresholds and withdrawal latencies to heat were determined after i.t. administration of nicotine, a non-specific nAChR agonist. In WT mice (Fig. 3A), a low dose, but not a high dose, of nicotine increased mechanical paw withdrawal threshold ($F_{2,11} = 5.32$, $p = 0.02$) and withdrawal latencies to heat ($F_{2,16} = 3.07$, $p = 0.07$, Fig. 3C) as compared to vehicle (saline) control. In the *tmem35a* KO mice, neither nicotine doses altered withdrawal responses to mechanical stimuli (time x nicotine dose interaction, $F_{8, 44} = 0.22$, $p = 0.99$, Fig. 3B), and only a high dose of nicotine produced analgesia to heat stimuli which persisted for >30 min (time x nicotine dose interaction, $F_{8,76} = 3.58$, $p = 0.0014$, Fig. 3D). Administration of vehicle did not alter withdrawal latencies to heat at any time.

Effects of the nAChRα7-specific agonist, PHA543613, on mechanical and heat sensitivity in WT and tmem35a KO mice

To test the specific role of spinal cord α7 nAChR in *tmem35a* KO mice, effects of i.t. administration of the α7-specific agonist, PHA543613 (PHA) on withdrawal responses to mechanical and heat stimuli were determined. Based on an estimated ED_{50} of 65 nM PHA for α7–$5HT_3$ chimera (Wishka et al. 2006) and the high affinity of PHA for α7 ($K_i = 8.8$ nM) over α4β2 and $5HT_3$ receptors (Toyohara and Hashimoto 2010), PHA doses of 10 and 50 nM were used. The effects of PHA on mechanical (Fig. 4A–B) and heat sensitivity (Fig. 4C–D) were dose-dependent. Whereas a 10 nM dose of PHA produced analgesia to mechanical stimuli in WT ($F_{2,12} = 3.68$, $p = 0.057$), a 50 nM dose of PHA was needed to increase withdrawal threshold in KO mice (PHA x time interaction, $F_{8,48} = 2.70$, $p = 0.016$). Similarly, PHA produced analgesia to heat stimuli in WT mice (PHA x time interaction, $F_{8,48} = 3.10$, $p = 0.007$), but not in KO mice at either dose (PHA x time interaction, $F_{8,60} = 1.22$, $p = 0.305$).

Spinal cord transcriptome reveals increased inflammatory activity in tmem35 KO mice

To gain further insights into the molecular mechanisms underlying the hyperalgesia in *tmem35a* KO mice, an unbiased transcriptomic approach was performed. RNAseq analysis (n=4/genotype) revealed 72 differentially-expressed genes (DEGs) between *tmem35a* KO and WT mice, with 39 down- and 33 up-regulated genes in the spinal cord (Table). Notably, the spinal cord of *tmem35a* KO mice had lower expression of *fosB* ($\log_2$[Fold Change, FC] $= -0.91$, $p<0.0001$), serotonin receptor 3a (*Htr3a*, $\log_2 FC = -0.70$, $p = 0.0001$), and prodynorphin (*Pdyn*, $\log_2 FC = -0.58$, $p = 0.0003$) concomitant with a higher expression of S100 calcium binding protein A8 and A9 ($\mathrm{Log}_2 FC = +1.94$ and $+1.67$, $p < 0.0001$) and neuropeptide S receptor 1 (*Npsr1*, $\log_2 FC = +1.12$, $p < 0.0001$). Using the knowledge-based database (Ingenuity Pathway Analysis) these 72 DEGs were mapped onto known biological functions. Several themes emerged from these data and include reduced activity of intracellular transport of molecules, reduced neuroglia activation, increased inflammation, and increased inflammatory cell number (Fig. 5A). These DEGs also predicted corresponding increased activity of upstream regulators implicated in proinflammation (i.e., TCF7L2, AIRE, EHF) and decreased activity of anti-inflammatory factors (i.e., IKBKB, CHUK, Fig. 5B). To validate the predictive increased number of immune cells, cells immune-reactive for ionized calcium binding adaptor molecule 1 (Iba1), a specific marker for microglia/macrophage, were estimated by quantifying Iba1$^+$ cells across representative sections (n=3/mouse, 5WT, 4KO) of the dorsal horn lamina I through III (Fig. 5C). The mean number of Iba1$^+$ cells were 11.8 (± 1.3) and 18.5 (± 1.3) cells/section for WT and KO mice, respectively, (Fig. 5C, $p = 0.009$, $t = 3.6$, $df = 7$).

Discussion

The present study demonstrates that genetic deletion of *tmem35a* results in the development of mechanical allodynia and hyperalgesia to heat and cold stimuli. A role for NACHO in the modulation of pain at the spinal level was further supported by the absence of analgesia following intrathecal administration of nicotine or PHA in *tmem35a* KO mice at doses that produced analgesia in WT mice. Given the newly discovered role of *tmem35a*-encoding protein, or NACHO, as a major chaperone for the assembly and trafficking of neuronal homomeric α7 in particular, and to a lesser extent for the heteromeric α3, α4, and α6-containing nAChR subtypes, our findings highlight an important role for spinal neuronal α7 in nociception. Further analysis of the underlying molecular changes in spinal cord transcriptome in *tmem35a* KO mice suggest that the absence of NACHO leads to a heightened state of neuroinflammation corroborated by an increased number of microglia in the dorsal horn. The contribution of glia activation in the spinal cord to central sensitization and pain is well known (Chen et al. 2018; Ji et al. 2016), however, it is not clear whether a loss of neuronal α7 nAChR activity in *tmem35a* KO mice alters the mechanisms by which glia activation produces pain. Further studies are needed to elucidate this crosstalk. Collectively, results from the present study support important roles for neuronal-specific NACHO in pain processing.

Mechanical allodynia and hyperalgesia to heat and cold stimuli in *tmem35a* KO mice suggest that neuronal α7, and to a lesser extent α3, α4, and α6-containing receptor subtypes, is dependent on its trafficking and assembly by NACHO. The absence of analgesia to heat following intrathecal PHA in *tmem35a* KO mice suggests that neuronal α7 nAChR is essential for modulating information related to noxious heat, confirming an earlier study that used selective agonist/antagonist in preclinical pain models (Rowley et al. 2008). Interestingly, analgesia to noxious heat was observed with a high dose of intrathecal nicotine in the KO mice. This observation suggests a possibility that activation of limited residual α3, α4 and α6-containing receptor subtypes in the *tmem35a* KO would require a nicotine dose that normally induces receptor desensitization in WT mice (Kem et al. 2018; Khan et al. 1998; López-Hernández et al. 2009).

The mechanisms underlying mechanical allodynia in *tmem35* KO mice are unclear. One possibility is that reduced activity of neuronal α3, α4, and α6-containing receptor subtypes contributes to mechanical allodynia. While in vitro evidence supports the role of NACHO in the assembly and expression of these receptors, the residual binding of their selective agonists (i.e., epibatidine and conotoxin II) in the brain of tmem35a KO mouse suggests at least a partial conservation of receptor function (Deshpande et al. 2020; Gu et al. 2016;

Matta et al. 2017). This would be consistent with the implicated roles of these receptors in the modulation of mechanical allodynia at the spinal cord level (Rowley et al. 2008; Wieskopf et al. 2015; Young et al. 2008). Thus, the observed mitigation of mechanical allodynia following a high dose of PHA543613 in the *tmem35a* KO mice suggests that residual α3, α4, and α6 could be activated with a high dose of the α7 selective agonist. Another possibility is that activation of glial α7 nAChR in the spinal cord by PHA543613 might attenuate mechanical allodynia in *tmem35* KO mice. Indeed, intrathecal administration of selective α7 agonists activate microglial anti-inflammatory activity by inhibiting pro-inflammatory cytokine (e.g., IL1β) production, and reduced mechanical allodynia in rat models of post-traumatic stress disorder and HIV-related inflammatory pain (Loram et al. 2010; Sun et al. 2017). Consistent with this notion, our preliminary data (not shown) indicate a functional preservation of microglial α7 nAChR in *tmem35a* KO mice evidenced by the presence of transcriptional responses of microglial-specific downstream target genes (e.g., *IL1β*, *Tnfα*, and S100B (Dash et al. 2016; Huang et al. 2013)) and the absence of neuronal-specific responses (e.g., *c-fos and Egr1* (Thomsen et al. 2008; Vazquez-Padron et al. 2010)) immediately following intranasal PHA. This possibility is also in line with the RNAseq data indicating increased neuroinflammation in the KO mouse spinal cord.

It is also possible that increased pain sensitivity in *tmem35* KO NACHO could result from reduced GABAergic inhibition in the spinal cord. While NACHO is important for neuronal activity of α7, it is also involved in the assembly and trafficking of α4-containing receptors (Gu et al. 2016; Matta et al. 2017). This could impair the spinal cord GABAergic inhibitory tone as these neurons possess α4-containing receptors (Cordero-Erausquin et al. 2004; Rashid et al. 2006). Reduced Ca^{2+} currents in these neurons may lead to less inhibitory modulation (Du et al. 2017; Umana et al. 2013).

In addition, intracellular signaling pathways mediated by Ca^{2+}entry are important for the development of pathological pain via activation of canonical calcium-dependent (e.g. CaMKs) mechanisms that regulate transcription of relevant gene targets (e.g., *Pdyn, CaMKIV, Creb, and C1q*) (Cavanaugh et al. 2011; D'Arco et al. 2015; Guo et al. 2004; Hagenston and Simonetti 2014; Lalisse et al. 2018; Luo et al. 2008; Matsumura et al. 2015; Schlumm et al. 2013; Simonetti et al. 2013; Stemkowski et al. 2016). Reduced neuronal Ca^{2+}entry could produce similar gene dysregulation in the *tmem35a* KO spinal cord. Indeed, the transcriptomic findings in the spinal cord of *tmem35a* KO mice showed consistent changes in regulation of the aforementioned genes. Our transcriptomic data also showed an altered profile of receptors and nociceptive signaling molecules in the spinal cord of *tmem35a* KO mice. For example, reduced expression of *Htr3a*, *fosB*, and *Pdyn* (see Table) could be associated with hyperalgesia in these mice as they have been implicated in various pain models (Knisely et al. 2019; Negrete et al. 2017; Solecki et al. 2008; Tang et al. 2020; Tesarz et al. 2013; Wang et al. 2001). While the role of *Htr3a*-encoding peptide 5-HT_3R in the spinal cord remains unclear with evidence both supporting and against its antinociceptive activity (Costa-Pereira et al. 2020; Khasabov et al. 1999; Raithel et al. 2018; Tang et al. 2020), a lower level of *Htr3a* coupled with the hyperalgesia in the *tmem35a* KO mice support an anti-nociceptive role for this receptor in neurons. Likewise, reduced *fosB* expression, a transcriptional regulator highly expressed in immune cells, could also have compensatory implications. FOSB can induce NF-kB expression and associated inflammatory response, and increased expression of *fosB* in the spinal cord has been associated with the development of chronic pain (Dimitrov et al. 2014; Luis-Delgado et al. 2006; McClung and Nestler 2003; Tesarz et al. 2013). Nonetheless, our finding suggests an antinociceptive role of FOSB or a compensatory gene transcriptional response induced by the pain phenotype in KO mice. Similarly, neuropathic pain was associated with upregulation of spinal cord prodynorphin (*Pdyn*), a preprotein of a secreted peptide for kappa-opioid receptor expressed in lamina I of the dorsal horn (Ji et al. 2019; Wang et al. 2001). Contrary to these observations, *Pdyn* KO mice exhibited mechanical allodynia associated with inflammatory pain (Negrete et al. 2017). Our findings of reduced spinal cord *Pdyn* expression concomitant with the mechanical allodynia in *tmem35* KO mice support an antinociceptive function of prodynorphin.

Analysis of differentially-expressed genes by IPA predicted increased neuroinflammation in the KO mouse. This effect is consistent with the elevated immune responses found in α4, β2, and α7 KO mice (Fujii et al. 2007; Skok et al. 2005). The underlying mechanism for this neuron-microglia crosstalk mediated by nAChR remains to be determined. However, the altered expression of genes known to be highly expressed in immune cells (e.g., S100A8/9, SEMA4D, KLK6) highlights the importance of neuronal nAChRs in mediating neuron-microglia interactions. S100A8/9 are calcium binding proteins that are found predominantly in myeloid cells and circulating neutrophils and have been implicated in pro-inflammatory response and inflammatory pain (Roth et al. 2003; Sunahori et al. 2006). SEMA4D is a secreted peptide which is found primarily in leukocytes, that has been shown to facilitate dendritic and axonal morphogenesis through activation of neuronal plexin receptors (Hall et al. 1996; Vodrazka et al. 2009). Increased SEMA4D activity was associated with neuropathic pain (Binmadi et al. 2012; Gong et al. 2019). KLK6, a member of serine proteolytic family expressed in oligodendrocytes and macrophages, has been implicated in inflammatory responses following insults of the central nervous system (Scarisbrick et al. 2006; Yoshida 2003). Increased KLK6 expression could facilitate microglial mobilization in the spinal cord (Ghosh et al. 2004). These transcriptional changes could contribute to pain hypersensitivity in *tmem35a* KO mice.

In summary, we found that mice with loss of neuronal-specific NACHO exhibited mechanical allodynia and thermal hyperalgesia. This phenotype was associated with a loss of α7 or reduced neuronal activity of α3, α4, and α6-containing nAChR subtypes accompanied by molecular changes in the spinal cord indicative of neuroinflammation. Although these findings highlight the contribution of NACHO-expressing neurons in the spinal cord to the modulation of pain, future studies are needed to unravel the underlying molecular mechanisms.

Acknowledgments:

We thank Dr. Michael Georgieff for his generosity in financial support via the Harrison Chair Endowment to continue this important research. We thank Dr. Ralph Loring (Northeastern University) for his contribution in reviewing and editing our manuscript.

Grants: This work was supported by the Vikings' Children Fund and Minnesota Medical Foundation to P.V.T., and NIH grants CA241627 and HL135895 to D.A.S.

Abbreviations

NACHO	Novel Acetylcholine receptor Chaperone
nAChR	nicotinic acetylcholine receptor
CGRP	Calcitonin gene-related peptide
IB4	Isolectin B4
IPA	Ingenuity Pathway Analysis

References

Aceto MD, Bagley RS, Dewey WL, Fu TC, and Martin BR. The Spinal-Cord as a Major Site for the Antinociceptive Action of Nicotine in the Rat. Neuropharmacology 25: 1031–1036, 1986. [PubMed: 3774124]

AlSharari SD, Carroll FI, McIntosh JM, and Damaj MI. The antinociceptive effects of nicotinic partial agonists varenicline and sazetidine-A in murine acute and tonic pain models. The Journal of pharmacology and experimental therapeutics 342: 742–749, 2012. [PubMed: 22678099]

Alsharari SD, Freitas K, and Damaj MI. Functional role of alpha7 nicotinic receptor in chronic neuropathic and inflammatory pain: studies in transgenic mice. Biochemical pharmacology 86: 1201–1207, 2013. [PubMed: 23811428]

Barks A, Fretham SJB, Georgieff MK, and Tran PV. Early-Life Neuronal-Specific Iron Deficiency Alters the Adult Mouse Hippocampal Transcriptome. J Nutr 148: 1521–1528, 2018. [PubMed: 30169712]

Bertrand D, and Terry AV Jr. The wonderland of neuronal nicotinic acetylcholine receptors. Biochemical pharmacology 151: 214–225, 2018. [PubMed: 29248596]

Binmadi NO, Yang Y-H, Zhou H, Proia P, Lin Y-L, De Paula AMB, Guimarães ALS, Poswar FO, Sundararajan D, and Basile JR. Plexin-B1 and semaphorin 4D cooperate to promote perineural invasion in a RhoA/ROK-dependent manner. Am J Pathol 180: 1232–1242, 2012. [PubMed: 22252234]

Cavanaugh DJ, Chesler AT, Jackson AC, Sigal YM, Yamanaka H, Grant R, O’Donnell D, Nicoll RA, Shah NM, Julius D, and Basbaum AI. Trpv1 reporter mice reveal highly restricted brain distribution and functional expression in arteriolar smooth muscle cells. The Journal of neuroscience : the official journal of the Society for Neuroscience 31: 5067–5077, 2011.

Chaplan SR, Bach FW, Pogrel JW, Chung JM, and Yaksh TL. Quantitative assessment of tactile allodynia in the rat paw. Journal of Neuroscience Methods 53: 55–63, 1994. [PubMed: 7990513]

Chen G, Zhang YQ, Qadri YJ, Serhan CN, and Ji RR. Microglia in Pain: Detrimental and Protective Roles in Pathogenesis and Resolution of Pain. Neuron 100: 1292–1311, 2018. [PubMed: 30571942]

Christensen MK, and Smith DF. Antinociceptive effects of the stereoisomers of nicotine given intrathecally in spinal rats. J Neural Transm Gen Sect 80: 189–194, 1990. [PubMed: 2158797]

Cordero-Erausquin M, Pons S, Faure P, and Changeux JP. Nicotine differentially activates inhibitory and excitatory neurons in the dorsal spinal cord. Pain 109: 308–318, 2004. [PubMed: 15157692]

Costa-Pereira JT, Serrão P, Martins I, and Tavares I. Serotoninergic pain modulation from the rostral ventromedial medulla (RVM) in chemotherapy-induced neuropathy: The role of spinal 5-HT3 receptors. The European journal of neuroscience 51: 1756–1769, 2020. [PubMed: 31691396]

Crespi A, Colombo SF, and Gotti C. Proteins and chemical chaperones involved in neuronal nicotinic receptor expression and function: an update. Br J Pharmacol 2017.

D’Arco M, Margas W, Cassidy JS, and Dolphin AC. The upregulation of alpha2delta-1 subunit modulates activity-dependent Ca2+ signals in sensory neurons. The Journal of neuroscience : the official journal of the Society for Neuroscience 35: 5891–5903, 2015. [PubMed: 25878262]

Dahlhamer J, Lucas J, Zelaya C, Nahin R, Mackey S, DeBar L, Kerns R, Von Korff M, Porter L, and Helmick C. Prevalence of Chronic Pain and High-Impact Chronic Pain Among Adults - United States, 2016. MMWR Morb Mortal Wkly Rep 67: 1001–1006, 2018. [PubMed: 30212442]

Dash PK, Zhao J, Kobori N, Redell JB, Hylin MJ, Hood KN, and Moore AN. Activation of Alpha 7 Cholinergic Nicotinic Receptors Reduce Blood-Brain Barrier Permeability following Experimental Traumatic Brain Injury. The Journal of neuroscience : the official journal of the Society for Neuroscience 36: 2809–2818, 2016. [PubMed: 26937017]

Deshpande A, Vinayakamoorthy RM, Garg BK, Thummapudi JP, Oza G, Adhikari K, Agarwal A, Dalvi P, Iyer S, Thulasi Raman S, Ramesh V, Rameshbabu A, Rezvaya A, Sukumaran S, Swaminathan S, Tilak B, Wang Z, Tran PV, and Loring RH. Why Does Knocking Out NACHO, But Not RIC3, Completely Block Expression of α7 Nicotinic Receptors in Mouse Brain? Biomolecules 10: 2020.

Dimitrov EL, Tsuda MC, Cameron HA, and Usdin TB. Anxiety- and depression-like behavior and impaired neurogenesis evoked by peripheral neuropathy persist following resolution of prolonged tactile hypersensitivity. The Journal of neuroscience : the official journal of the Society for Neuroscience 34: 12304–12312, 2014. [PubMed: 25209272]

Ditre JW, Zale EL, LaRowe LR, Kosiba JD, and De Vita MJ. Nicotine deprivation increases pain intensity, neurogenic inflammation, and mechanical hyperalgesia among daily tobacco smokers. J Abnorm Psychol 127: 578–589, 2018. [PubMed: 29781659]

Du X, Hao H, Yang Y, Huang S, Wang C, Gigout S, Ramli R, Li X, Jaworska E, Edwards I, Deuchars J, Yanagawa Y, Qi J, Guan B, Jaffe DB, Zhang H, and Gamper N. Local GABAergic signaling within sensory ganglia controls peripheral nociceptive transmission. J Clin Invest 127: 1741–1756, 2017. [PubMed: 28375159]

Enna SJ, and McCarson KE. The role of GABA in the mediation and perception of pain. Advances in pharmacology (San Diego, Calif) 54: 1–27, 2006.

Feuerbach D, Lingenhoehl K, Olpe HR, Vassout A, Gentsch C, Chaperon F, Nozulak J, Enz A, Bilbe G, McAllister K, and Hoyer D. The selective nicotinic acetylcholine receptor alpha7 agonist JN403 is active in animal models of cognition, sensory gating, epilepsy and pain. Neuropharmacology 56: 254–263, 2009.

Flood P, and Daniel D. Intranasal nicotine for postoperative pain treatment. Anesthesiology 101: 1417–1421, 2004. [PubMed: 15564950]

Freitas KC, Carroll FI, and Negus SS. Effects of nicotinic acetylcholine receptor agonists in assays of acute pain-stimulated and pain-depressed behaviors in rats. The Journal of pharmacology and experimental therapeutics 355: 341–350, 2015. [PubMed: 26359313]

Fujii YX, Fujigaya H, Moriwaki Y, Misawa H, Kasahara T, Grando SA, and Kawashima K. Enhanced serum antigen-specific IgG1 and proinflammatory cytokine production in nicotinic acetylcholine receptor alpha7 subunit gene knockout mice. J Neuroimmunol 189: 69–74, 2007. [PubMed: 17675251]

Gao B, Hierl M, Clarkin K, Juan T, Nguyen H, Valk M, Deng H, Guo W, Lehto SG, Matson D, McDermott JS, Knop J, Gaida K, Cao L, Waldon D, Albrecht BK, Boezio AA, Copeland KW, Harmange JC, Springer SK, Malmberg AB, and McDonough SI. Pharmacological effects of nonselective and subtype-selective nicotinic acetylcholine receptor agonists in animal models of persistent pain. Pain 149: 33–49, 2010. [PubMed: 20167427]

Gaskin DJ, and Richard P. The economic costs of pain in the United States. The journal of pain : official journal of the American Pain Society 13: 715–724, 2012.

Genzen JR, and McGehee DS. Nicotinic modulation of GABAergic synaptic transmission in the spinal cord dorsal horn. Brain Res 1031: 229–237, 2005. [PubMed: 15649448]

Ghosh MC, Grass L, Soosaipillai A, Sotiropoulou G, and Diamandis EP. Human kallikrein 6 degrades extracellular matrix proteins and may enhance the metastatic potential of tumour cells. Tumour Biol 25: 193–199, 2004. [PubMed: 15557757]

Gong H, Lyu X, Li S, Chen R, Hu M, and Zhang X. sSema4D levels are increased in coronary heart disease and associated with the extent of coronary artery stenosis. Life Sci 219: 329–335, 2019. [PubMed: 30658102]

Gonzalez-Islas C, Garcia-Bereguiain MA, O'Flaherty B, and Wenner P. Tonic nicotinic transmission enhances spinal GABAergic presynaptic release and the frequency of spontaneous network activity. Dev Neurobiol 76: 298–312, 2016. [PubMed: 26061781]

Gu S, Matta JA, Lord B, Harrington AW, Sutton SW, Davini WB, and Bredt DS. Brain alpha7 Nicotinic Acetylcholine Receptor Assembly Requires NACHO. Neuron 89: 948–955, 2016. [PubMed: 26875622]

Guo W, Wei F, Zou S, Robbins MT, Sugiyo S, Ikeda T, Tu JC, Worley PF, Dubner R, and Ren K. Group I metabotropic glutamate receptor NMDA receptor coupling and signaling cascade mediate spinal dorsal horn NMDA receptor 2B tyrosine phosphorylation associated with inflammatory hyperalgesia. The Journal of neuroscience : the official journal of the Society for Neuroscience 24: 9161–9173, 2004. [PubMed: 15483135]

Hagenston AM, and Simonetti M. Neuronal calcium signaling in chronic pain. Cell and tissue research 357: 407–426, 2014. [PubMed: 25012522]

Hall KT, Boumsell L, Schultze JL, Boussiotis VA, Dorfman DM, Cardoso AA, Bensussan A, Nadler LM, and Freeman GJ. Human CD100, a novel leukocyte semaphorin that promotes B-cell aggregation and differentiation. Proceedings of the National Academy of Sciences of the United States of America 93: 11780–11785, 1996. [PubMed: 8876214]

Hama AT, Lloyd GK, and Menzaghi F. The antinociceptive effect of intrathecal administration of epibatidine with clonidine or neostigmine in the formalin test in rats. Pain 91: 131–138, 2001. [PubMed: 11240085]

Hamamoto DT, Giridharagopalan S, and Simone DA. Acute and chronic administration of the cannabinoid receptor agonist CP 55,940 attenuates tumor-evoked hyperalgesia. European journal of pharmacology 558: 73–87, 2007. [PubMed: 17250825]

Holtman JR Jr., Crooks PA, Johnson-Hardy JK, and Wala EP. The analgesic and toxic effects of nornicotine enantiomers alone and in interaction with morphine in rodent models of acute and persistent pain. Pharmacol Biochem Behav 94: 352–362, 2010. [PubMed: 19800911]

Huang SH, Wang L, Chi F, Wu CH, Cao H, Zhang A, and Jong A. Circulating brain microvascular endothelial cells (cBMECs) as potential biomarkers of the blood-brain barrier disorders caused by microbial and non-microbial factors. PloS one 8: e62164, 2013. [PubMed: 23637989]

Hwang JH, and Yaksh TL. The effect of spinal GABA receptor agonists on tactile allodynia in a surgically-induced neuropathic pain model in the rat. Pain 70: 15–22, 1997. [PubMed: 9106805]

Hylden JL, and Wilcox GL. Intrathecal morphine in mice: a new technique. Eur J Pharmacol 67: 313–316, 1980. [PubMed: 6893963]

Jamner LD, Girdler SS, Shapiro D, and Jarvik ME. Pain inhibition, nicotine, and gender. Exp Clin Psychopharmacol 6: 96–106, 1998. [PubMed: 9526150]

Jareczek FJ, White SR, and Hammond DL. Plasticity in Brainstem Mechanisms of Pain Modulation by Nicotinic Acetylcholine Receptors in the Rat. eNeuro 4: 2017.

Ji L, Chen Y, Wei H, Feng H, Chang R, Yu D, Wang X, Gong X, and Zhang M. Activation of alpha7 acetylcholine receptors reduces neuropathic pain by decreasing dynorphin A release from microglia. Brain Res 1715: 57–65, 2019. [PubMed: 30898676]

Ji RR, Chamessian A, and Zhang YQ. Pain regulation by non-neuronal cells and inflammation. Science 354: 572–577, 2016. [PubMed: 27811267]

Kabbani N, and Nichols RA. Beyond the Channel: Metabotropic Signaling by Nicotinic Receptors. Trends in pharmacological sciences 39: 354–366, 2018. [PubMed: 29428175]

Kem WR, Olincy A, Johnson L, Harris J, Wagner BD, Buchanan RW, Christians U, and Freedman R. Pharmacokinetic Limitations on Effects of an Alpha7-Nicotinic Receptor Agonist in Schizophrenia: Randomized Trial with an Extended-Release Formulation. Neuropsychopharmacology 43: 583–589, 2018. [PubMed: 28825423]

Kennedy BC, Dimova JG, Dakoji S, Yuan LL, Gewirtz JC, and Tran PV. Deletion of novel protein TMEM35 alters stress-related functions and impairs long-term memory in mice. American journal of physiology Regulatory, integrative and comparative physiology 311: R166–178, 2016.

Kesingland AC, Gentry CT, Panesar MS, Bowes MA, Vernier JM, Cube R, Walker K, and Urban L. Analgesic profile of the nicotinic acetylcholine receptor agonists, (+)-epibatidine and ABT-594 in models of persistent inflammatory and neuropathic pain. Pain 86: 113–118, 2000. [PubMed: 10779668]

Khan IM, Buerkle H, Taylor P, and Yaksh TL. Nociceptive and antinociceptive responses to intrathecally administered nicotinic agonists. Neuropharmacology 37: 1515–1525, 1998. [PubMed: 9886674]

Khasabov SG, Lopez-Garcia JA, Asghar AU, and King AE. Modulation of afferent-evoked neurotransmission by 5-HT3 receptors in young rat dorsal horn neurones in vitro: a putative mechanism of 5-HT3 induced anti-nociception. Br J Pharmacol 127: 843–852, 1999. [PubMed: 10433490]

Khasabov SG, Malecha P, Noack J, Tabakov J, Giesler GJ Jr., and Simone DA. Hyperalgesia and sensitization of dorsal horn neurons following activation of NK-1 receptors in the rostral ventromedial medulla. Journal of neurophysiology 118: 2727–2744, 2017. [PubMed: 28794197]

Kiguchi N, Kobayashi D, Saika F, Matsuzaki S, and Kishioka S. Inhibition of peripheral macrophages by nicotinic acetylcholine receptor agonists suppresses spinal microglial activation and neuropathic pain in mice with peripheral nerve injury. J Neuroinflammation 15: 96–96, 2018. [PubMed: 29587798]

Knisely MR, Conley YP, Smoot B, Paul SM, Levine JD, and Miaskowski C. Associations Between Catecholaminergic and Serotonergic Genes and Persistent Arm Pain Severity Following Breast Cancer Surgery. The journal of pain : official journal of the American Pain Society 20: 1100–1111, 2019.

Lalisse S, Hua J, Lenoir M, Linck N, Rassendren F, and Ulmann L. Sensory neuronal P2RX4 receptors controls BDNF signaling in inflammatory pain. Scientific reports 8: 964, 2018. [PubMed: 29343707]

Larsson M, and Broman J. Synaptic plasticity and pain: role of ionotropic glutamate receptors. The Neuroscientist : a review journal bringing neurobiology, neurology and psychiatry 17: 256–273, 2011.

López-Hernández GY, Thinschmidt JS, Morain P, Trocme-Thibierge C, Kem WR, Soti F, and Papke RL. Positive modulation of alpha7 nAChR responses in rat hippocampal interneurons to full agonists and the alpha7-selective partial agonists, 4OH-GTS-21 and S 24795. Neuropharmacology 56: 821–830, 2009. [PubMed: 19705574]

Loram LC, Harrison JA, Chao L, Taylor FR, Reddy A, Travis CL, Giffard R, Al-Abed Y, Tracey K, Maier SF, and Watkins LR. Intrathecal injection of an alpha seven nicotinic acetylcholine receptor agonist attenuates gp120-induced mechanical allodynia and spinal pro-inflammatory cytokine profiles in rats. Brain Behav Immun 24: 959–967, 2010. [PubMed: 20353818]

Loram LC, Taylor FR, Strand KA, Maier SF, Speake JD, Jordan KG, James JW, Wene SP, Pritchard RC, Green H, Van Dyke K, Mazarov A, Letchworth SR, and Watkins LR. Systemic administration of an alpha-7 nicotinic acetylcholine agonist reverses neuropathic pain in male Sprague Dawley rats. The journal of pain : official journal of the American Pain Society 13: 1162–1171, 2012.

Luis-Delgado OE, Barrot M, Rodeau J-L, Ulery PG, Freund-Mercier M-J, and Lasbennes F. The transcription factor DeltaFosB is recruited by inflammatory pain. J Neurochem 98: 1423–1431, 2006. [PubMed: 16787404]

Luo C, Seeburg PH, Sprengel R, and Kuner R. Activity-dependent potentiation of calcium signals in spinal sensory networks in inflammatory pain states. Pain 140: 358–367, 2008. [PubMed: 18926636]

Matsumura S, Taniguchi W, Nishida K, Nakatsuka T, and Ito S. In vivo two-photon imaging of structural dynamics in the spinal dorsal horn in an inflammatory pain model. The European journal of neuroscience 41: 989–997, 2015. [PubMed: 25645012]

Matta JA, Gu S, Davini WB, Lord B, Siuda ER, Harrington AW, and Bredt DS. NACHO Mediates Nicotinic Acetylcholine Receptor Function throughout the Brain. Cell reports 19: 688–696, 2017. [PubMed: 28445721]

Matthews AM, Fu R, Dana T, and Chou R. Intranasal or transdermal nicotine for the treatment of postoperative pain. Cochrane Database Syst Rev CD009634, 2016. [PubMed: 26756459]

Mazzaferro S, Whiteman ST, Alcaino C, Beyder A, and Sine SM. NACHO and 14–3-3 promote expression of distinct subunit stoichiometries of the α4β2 acetylcholine receptor. Cell Mol Life Sci 2020.

McClung CA, and Nestler EJ. Regulation of gene expression and cocaine reward by CREB and DeltaFosB. Nature neuroscience 6: 1208–1215, 2003. [PubMed: 14566342]

Medhurst SJ, Hatcher JP, Hille CJ, Bingham S, Clayton NM, Billinton A, and Chessell IP. Activation of the alpha7-nicotinic acetylcholine receptor reverses complete freund adjuvant-induced mechanical hyperalgesia in the rat via a central site of action. The journal of pain : official journal of the American Pain Society 9: 580–587, 2008.

Munro G, Hansen R, Erichsen H, Timmermann D, Christensen J, and Hansen H. The α7 nicotinic ACh receptor agonist compound B and positive allosteric modulator PNU-120596 both alleviate inflammatory hyperalgesia and cytokine release in the rat. Br J Pharmacol 167: 421–435, 2012. [PubMed: 22536953]

Negrete R, García Gutiérrez MS, Manzanares J, and Maldonado R. Involvement of the dynorphin/KOR system on the nociceptive, emotional and cognitive manifestations of joint pain in mice. Neuropharmacology 116: 315–327, 2017. [PubMed: 27567942]

Nirogi R, Goura V, Abraham R, and Jayarajan P. α4β2* neuronal nicotinic receptor ligands (agonist, partial agonist and positive allosteric modulators) as therapeutic prospects for pain. European journal of pharmacology 712: 22–29, 2013. [PubMed: 23660369]

Orr-Urtreger A, Broide RS, Kasten MR, Dang H, Dani JA, Beaudet AL, and Patrick JW. Mice homozygous for the L250T mutation in the alpha7 nicotinic acetylcholine receptor show increased neuronal apoptosis and die within 1 day of birth. J Neurochem 74: 2154–2166, 2000. [PubMed: 10800961]

Raithel SJ, Sapio MR, Iadarola MJ, and Mannes AJ. Thermal A-δ Nociceptors, Identified by Transcriptomics, Express Higher Levels of Anesthesia-Sensitive Receptors Than Thermal C-Fibers and Are More Suppressible by Low-Dose Isoflurane. Anesth Analg 127: 263–266, 2018. [PubMed: 28991117]

Rashid MH, Furue H, Yoshimura M, and Ueda H. Tonic inhibitory role of alpha4beta2 subtype of nicotinic acetylcholine receptors on nociceptive transmission in the spinal cord in mice. Pain 125: 125–135, 2006. [PubMed: 16781069]

Roth J, Vogl T, Sorg C, and Sunderkötter C. Phagocyte-specific S100 proteins: a novel group of proinflammatory molecules. Trends in immunology 24: 155–158, 2003. [PubMed: 12697438]

Rowbotham MC, Arslanian A, Nothaft W, Duan WR, Best AE, Pritchett Y, Zhou Q, and Stacey BR. Efficacy and safety of the α4β2 neuronal nicotinic receptor agonist ABT-894 in patients with diabetic peripheral neuropathic pain. Pain 153: 862–868, 2012. [PubMed: 22386472]

Rowley TJ, Payappilly J, Lu J, and Flood P. The antinociceptive response to nicotinic agonists in a mouse model of postoperative pain. Anesth Analg 107: 1052–1057, 2008. [PubMed: 18713928]

Saika F, Kiguchi N, Kobayashi Y, and Kishioka S. Peripheral alpha4beta2 nicotinic acetylcholine receptor signalling attenuates tactile allodynia and thermal hyperalgesia after nerve injury in mice. Acta physiologica (Oxford, England) 213: 462–471, 2015.

Scarisbrick IA, Sabharwal P, Cruz H, Larsen N, Vandell AG, Blaber SI, Ameenuddin S, Papke LM, Fehlings MG, Reeves RK, Blaber M, Windebank AJ, and Rodriguez M. Dynamic role of kallikrein 6 in traumatic spinal cord injury. The European journal of neuroscience 24: 1457–1469, 2006. [PubMed: 16987227]

Schlumm F, Mauceri D, Freitag HE, and Bading H. Nuclear calcium signaling regulates nuclear export of a subset of class IIa histone deacetylases following synaptic activity. The Journal of biological chemistry 288: 8074–8084, 2013. [PubMed: 23364788]

Simonetti M, Hagenston AM, Vardeh D, Freitag HE, Mauceri D, Lu J, Satagopam VP, Schneider R, Costigan M, Bading H, and Kuner R. Nuclear calcium signaling in spinal neurons drives a genomic program required for persistent inflammatory pain. Neuron 77: 43–57, 2013. [PubMed: 23312515]

Skok M, Grailhe R, and Changeux JP. Nicotinic receptors regulate B lymphocyte activation and immune response. European journal of pharmacology 517: 246–251, 2005. [PubMed: 15963492]

Solecki W, Krowka T, Kubik J, Kaczmarek L, and Przewlocki R. Increased analgesic tolerance to acute morphine in fosB knock-out mice: a gender study. Pharmacol Biochem Behav 90: 512–516, 2008. [PubMed: 18474394]

Stemkowski P, Garcia-Caballero A, Gadotti VM, M'Dahoma S, Huang S, Black SAG, Chen L, Souza IA, Zhang Z, and Zamponi GW. TRPV1 Nociceptor Activity Initiates USP5/T-type Channel-Mediated Plasticity. Cell reports 17: 2901–2912, 2016. [PubMed: 27974205]

Sullivan JP, Decker MW, Brioni JD, Donnelly-Roberts D, Anderson DJ, Bannon AW, Kang CH, Adams P, Piattoni-Kaplan M, Buckley MJ, and et al. (+/−)-Epibatidine elicits a diversity of in vitro and in vivo effects mediated by nicotinic acetylcholine receptors. The Journal of pharmacology and experimental therapeutics 271: 624–631, 1994. [PubMed: 7965777]

Sun R, Zhang W, Bo J, Zhang Z, Lei Y, Huo W, Liu Y, Ma Z, and Gu X. Spinal activation of alpha7-nicotinic acetylcholine receptor attenuates posttraumatic stress disorder-related chronic pain via suppression of glial activation. Neuroscience 344: 243–254, 2017. [PubMed: 28039041]

Sunahori K, Yamamura M, Yamana J, Takasugi K, Kawashima M, Yamamoto H, Chazin WJ, Nakatani Y, Yui S, and Makino H. The S100A8/A9 heterodimer amplifies proinflammatory cytokine production by macrophages via activation of nuclear factor kappa B and p38 mitogen-activated protein kinase in rheumatoid arthritis. Arthritis research & therapy 8: R69, 2006. [PubMed: 16613612]

Tang S, Jing H, Huang Z, Huang T, Lin S, Liao M, and Zhou J. Identification of key candidate genes in neuropathic pain by integrated bioinformatic analysis. J Cell Biochem 121: 1635–1648, 2020. [PubMed: 31535407]

Tesarz J, Hoheisel U, and Mense S. Tetrodotoxin-resistant fibres and spinal Fos expression: differences between input from muscle and skin. Exp Brain Res 224: 571–580, 2013. [PubMed: 23178907]

Thomsen MS, Mikkelsen JD, Timmermann DB, Peters D, Hay-Schmidt A, Martens H, and Hansen HH. The selective alpha7 nicotinic acetylcholine receptor agonist A-582941 activates immediate early genes in limbic regions of the forebrain: Differential effects in the juvenile and adult rat. Neuroscience 154: 741–753, 2008. [PubMed: 18495359]

Toyohara J, and Hashimoto K. α7 Nicotinic Receptor Agonists: Potential Therapeutic Drugs for Treatment of Cognitive Impairments in Schizophrenia and Alzheimer's Disease. The open medicinal chemistry journal 4: 37–56, 2010. [PubMed: 21249164]

Tran PV, Georgieff MK, and Engeland WC. Sodium Depletion Increases Sympathetic Neurite Outgrowth and Expression of a Novel TMEM35 Gene-Derived Protein (TUF1) in the Rat Adrenal Zona Glomerulosa. Endocrinology 2010.

Umana IC, Daniele CA, and McGehee DS. Neuronal nicotinic receptors as analgesic targets: it's a winding road. Biochemical pharmacology 86: 1208–1214, 2013. [PubMed: 23948066]

Umana IC, Daniele CA, Miller BA, Abburi C, Gallagher K, Brown MA, Mason P, and McGehee DS. Nicotinic modulation of descending pain control circuitry. Pain 158: 1938–1950, 2017. [PubMed: 28817416]

Vazquez-Padron RI, Mateu D, Rodriguez-Menocal L, Wei Y, Webster KA, and Pham SM. Novel role of Egr-1 in nicotine-related neointimal formation. Cardiovasc Res 88: 296–303, 2010. [PubMed: 20615913]

Vodrazka P, Korostylev A, Hirschberg A, Swiercz JM, Worzfeld T, Deng S, Fazzari P, Tamagnone L, Offermanns S, and Kuner R. The semaphorin 4D-plexin-B signalling complex regulates dendritic and axonal complexity in developing neurons via diverse pathways. The European journal of neuroscience 30: 1193–1208, 2009. [PubMed: 19788569]

Wang Z, Gardell LR, Ossipov MH, Vanderah TW, Brennan MB, Hochgeschwender U, Hruby VJ, Malan TP Jr., Lai J, and Porreca F Pronociceptive actions of dynorphin maintain chronic neuropathic pain. The Journal of neuroscience : the official journal of the Society for Neuroscience 21: 1779–1786, 2001. [PubMed: 11222667]

Wieskopf JS, Mathur J, Limapichat W, Post MR, Al-Qazzaz M, Sorge RE, Martin LJ, Zaykin DV, Smith SB, Freitas K, Austin JS, Dai F, Zhang J, Marcovitz J, Tuttle AH, Slepian PM, Clarke S, Drenan RM, Janes J, Al Sharari S, Segall SK, Aasvang EK, Lai W, Bittner R, Richards CI, Slade GD, Kehlet H, Walker J, Maskos U, Changeux JP, Devor M, Maixner W, Diatchenko L, Belfer I, Dougherty DA, Su AI, Lummis SC, Imad Damaj M, Lester HA, Patapoutian A, and Mogil JS. The nicotinic α6 subunit gene determines variability in chronic pain sensitivity via cross-inhibition of P2X2/3 receptors. Sci Transl Med 7: 287ra272, 2015.

Wishka DG, Walker DP, Yates KM, Reitz SC, Jia S, Myers JK, Olson KL, Jacobsen EJ, Wolfe ML, Groppi VE, Hanchar AJ, Thornburgh BA, Cortes-Burgos LA, Wong EHF, Staton BA, Raub TJ, Higdon NR, Wall TM, Hurst RS, Walters RR, Hoffmann WE, Hajos M, Franklin S, Carey G, Gold LH, Cook KK, Sands SB, Zhao SX, Soglia JR, Kalgutkar AS, Arneric SP, and Rogers BN. Discovery of N-[(3R)-1-Azabicyclo[2.2.2]oct-3-yl]furo[2,3-c]pyridine-5-carboxamide, an Agonist of the α7 Nicotinic Acetylcholine Receptor, for the Potential Treatment of Cognitive Deficits in Schizophrenia: Synthesis and Structure−Activity Relationship. Journal of Medicinal Chemistry 49: 4425–4436, 2006. [PubMed: 16821801]

Yoshida S Kallikrein-family serine protease in the central nervous system. Kaibogaku Zasshi 78: 77–82, 2003. [PubMed: 14531278]

Young T, Wittenauer S, McIntosh JM, and Vincler M. Spinal alpha3beta2* nicotinic acetylcholine receptors tonically inhibit the transmission of nociceptive mechanical stimuli. Brain Res 1229: 118–124, 2008. [PubMed: 18634758]

Author Manuscript

Author Manuscript

Author Manuscript

Highlights

- NACHO modulates spinal cord pain transmission
- Specific loss of neuronal α7 in *tmem35a* KO mice results in heat hyperalgesia
- The *tmem35a* KO spinal cord transcriptome indicates increased neuroinflammation

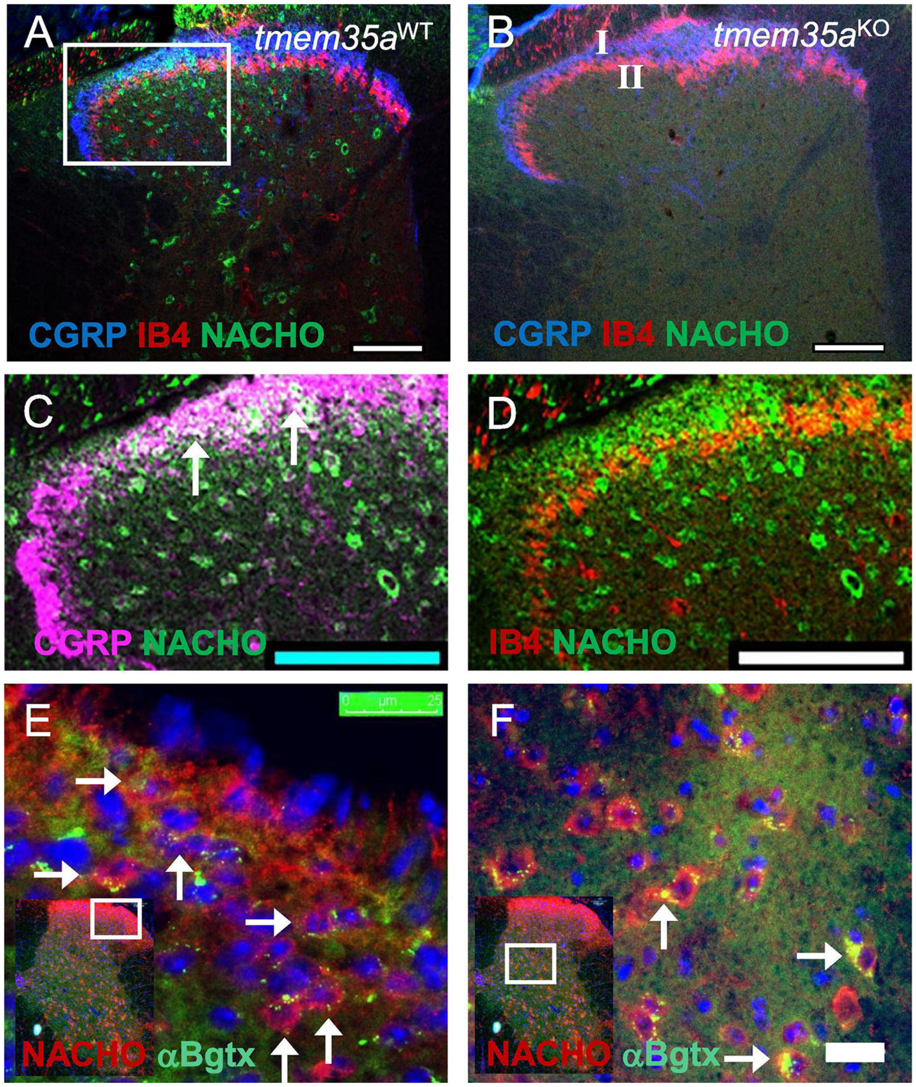

Figure 1:

NACHO expression in mouse dorsal spinal horn. (A) Confocal image of WT spinal cord showing NACHO$^+$ neurons (green), lamina I marked with CGRP$^+$ fiber (blue), and lamina II marked with IB4$^+$ fibers (red) of the dorsal horn. (B) Confocal image showing absence of NACHO$^+$ neurons in the *tmem35a* KO spinal cord without changes in the dorsal horn architecture. (C, D) Enlarged image of panel A (white box) showing colocalization of NACHO and peptidergic fibers in lamina I (panel C, CGRP$^+$, arrows), but little with non-peptidergic fibers (panel D, IB4$^+$) in lamina II. In panel C, the pseudocolor blue was converted to purple for visual enhancement of overlapping areas (white). (E, F) Photomicrographs showing colocalization of NACHO (red) and α7 nAChR (α-Bgtx, green) in lamina I, II (panel E) and V, VI (panel F). Cell nuclei were labeled with DAPI (blue) in panel E and F. White boxes in insets indicate enlarged areas of the dorsal horn. Scale bars = 100 μm for panel A and B, and 25 μm for panel E and F.

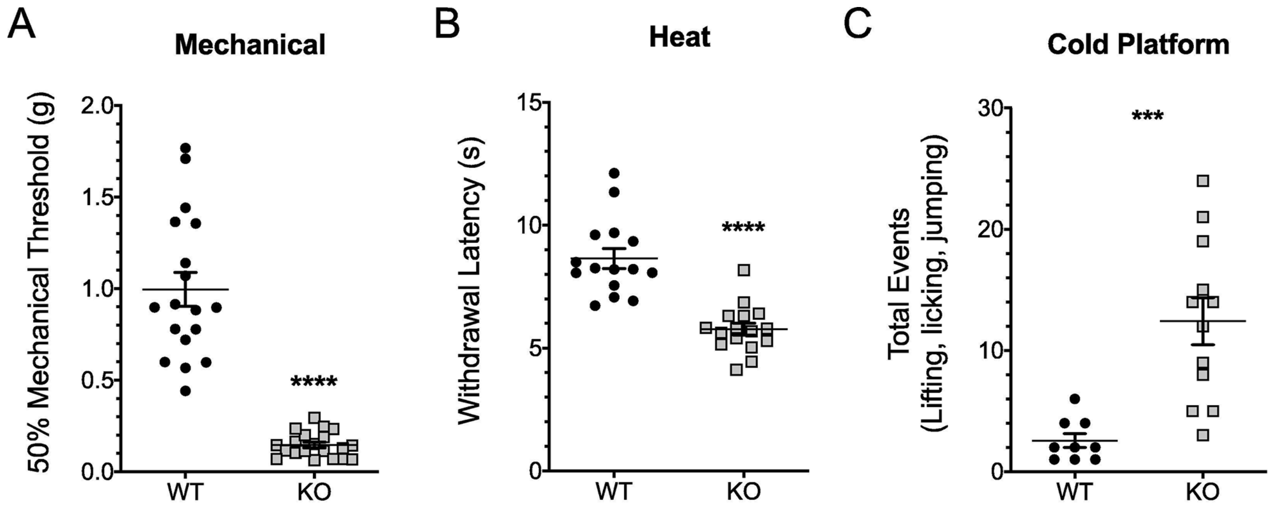

Figure 2:

Pain behaviors in *tmem35a* knockout (KO) adult male mice. KO mice showed hypersensitivity to mechanical (A) heat (B) and cold (C) stimuli as compared to WT control mice. Values are mean ± SEM, t-test, ***p<0.001, ****p<0.0001.

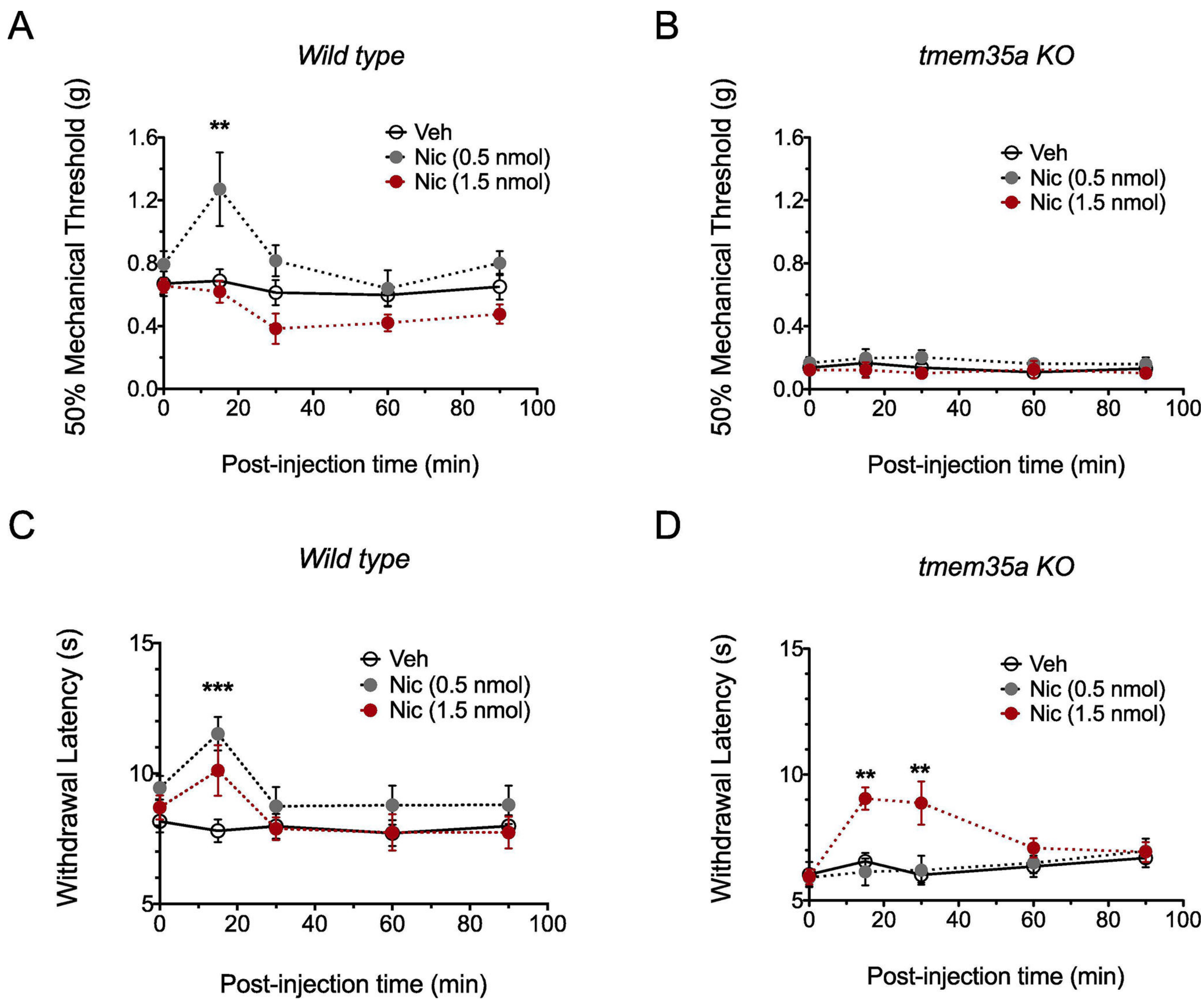

Figure 3:

Intrathecal administration nicotine produced analgesia to heat in *tmem35a* KO mice. In WT mice, nicotine (0.5 nmol) produced analgesia to mechanical and heat stimuli (panel A and C), but not at a higher (1.5 nmol) nicotine dose. In the KO mice, a high dose (1.5 nmol) of nicotine produced an analgesic response to heat, but not mechanical stimuli (panel B and D). Values are mean ± SEM, 2-way ANOVA with post hoc Bonferroni's multiple comparisons test, $^{**}p<0.01$, $^{***}p<0.001$.

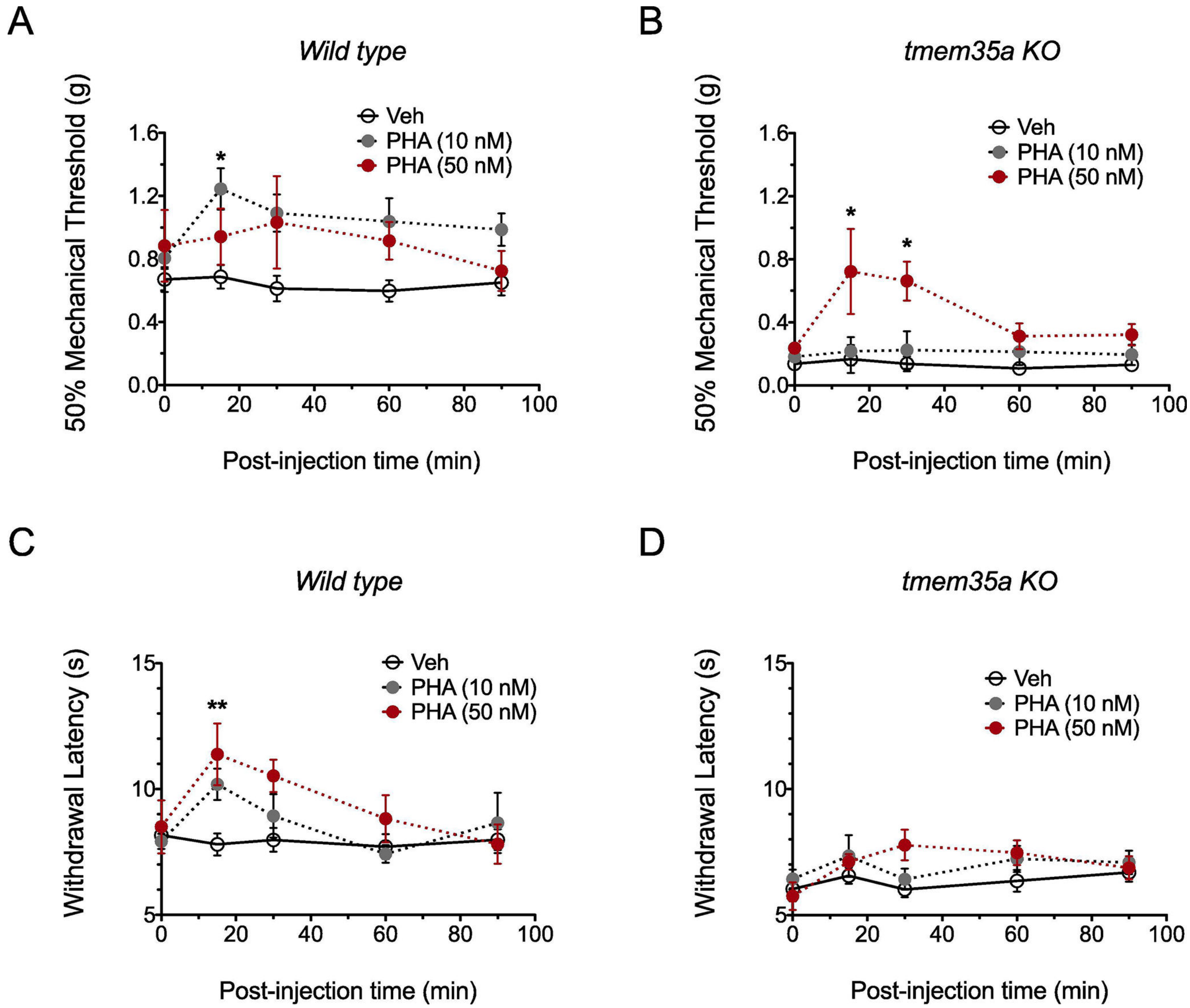

Figure 4:

High dose intrathecal PHA543613 administration reduced mechanical allodynia in *tmem35a* KO mice. In WT mice, PHA at doses of 10 nM or 50nM produced analgesia to mechanical and heat stimuli (A and C). In KO mice, only the 50 nM PHA dose reduced mechanical allodynia (B), whereas sensitivity to heat was not altered (D). Values are mean ± SEM, 2-way ANOVA with post hoc Bonferroni's multiple comparisons test, *p<0.05, **p<0.01.

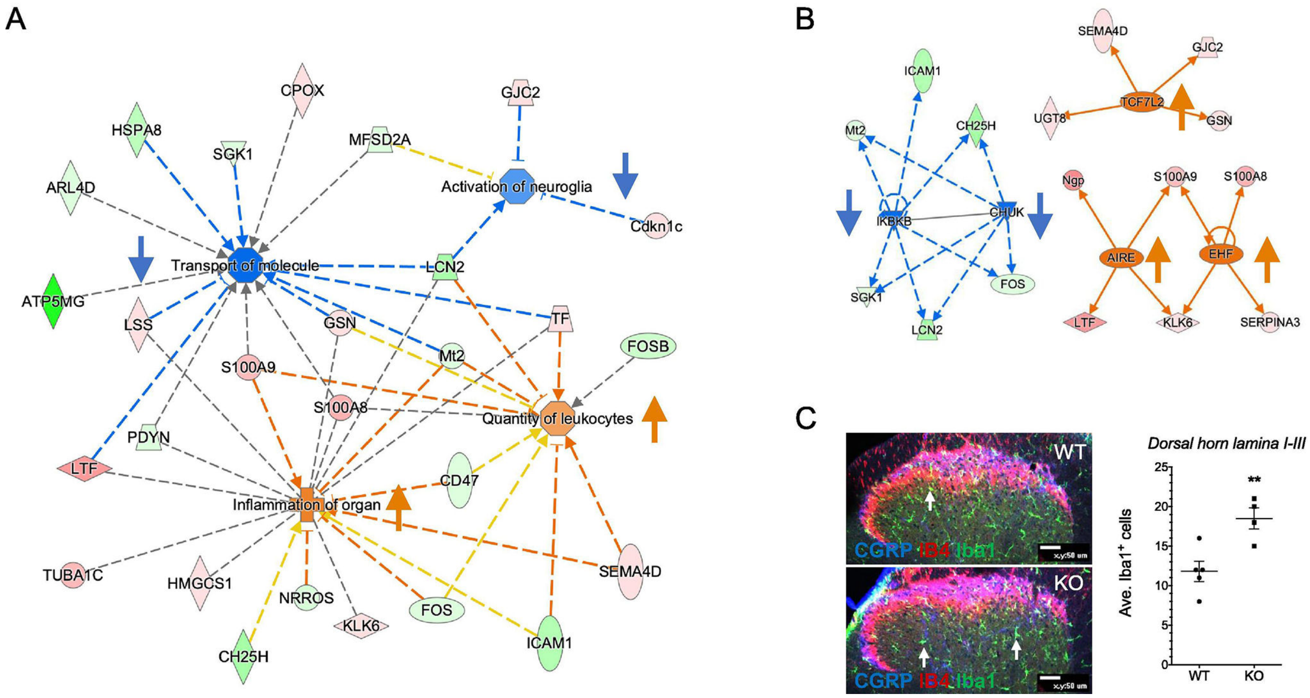

Figure 5:

Spinal cord transcriptomic analysis revealed increased neuro-inflammation in *tmem35a* KO mice. (A) A merged functional gene network showed a predictive reduction of intracellular transport of molecules (Z-score = −2.6, p = 0.0026) and neuroglia activation (Z-score = −1.0, p = 0.0005) concomitant with increased inflammation (Z-score = +1.4, p < 0.0001) and number of leukocytes (Z-score = +1.0, p = 0.0022). (B) Predictive activation of upstream regulators (e.g., TCF7L2, AIRE, and EHF, Z-score ≥ +2.0, p < 0.001) accompanied by reduced activity of inhibitors of inflammation (e.g., IKBKB, CHUK, Z-score < −2.2, p < 0.0001). Legends: Red/pink = upregulation, green = downregulation, orange line = leads to activation, blue line = leads to inhibition, yellow line = findings inconsistent with state of downstream molecule, and grey line = effect not predicted. Arrows indicate direction of change in activity. (C) Estimation of microglia (Iba1^{+}) in mouse spinal cord dorsal horn. Number of Iba1^{+} cells were counted in the dorsal horn lamina I through III using only visible cell bodies (arrows). Compared to WT, *tmem35a* KO mice showed a higher number of microglia in the dorsal horn. Representative confocal image of spinal cord dorsal horn labeled for CGRP (blue), IB4 (red), and Iba1 (green). Arrows indicate Iba1^{+} microglia. Scale bar = 50 μm. Values are mean ± SEM, t-test, **p<0.01.

Table 1

The 72 differentially-expressed genes in the *tmem35a* KO spinal cord.

Entrez Gene Name	ID	Log_2(KO/WT)	P-value	FDR (q-value)	Location	Type(s)
RIKEN cDNA 1700063D05 gene	1700063D05Rik	−1.43	0.00005	0.0131	Other	other
acid phosphatase 1	Acp1	0.596	0.00015	0.0316	Cytoplasm	phosphatase
actin alpha 1, skeletal muscle	Acta1	−0.764	0.00025	0.0483	Cytoplasm	other
aminoacylase 1	Acy1	−0.386	0.0001	0.0232	Cytoplasm	peptidase
ADP ribosylation factor like GTPase 4D	Arl4d	−0.578	0.00005	0.0131	Nucleus	enzyme
aryl hydrocarbon receptor nuclear translocator like 2	Arntl2	−1.655	0.00015	0.0316	Nucleus	transcription regulator
ATP synthase membrane subunit g	Atp5l	−4.132	0.00005	0.0131	Cytoplasm	enzyme
beaded filament structural protein 2	Bfsp2	1.697	0.00005	0.0131	Cytoplasm	other
calpain 11	Capn11	1.064	0.00005	0.0131	Cytoplasm	peptidase
carnosine synthase 1	Carns1	0.328	0.00005	0.0131	Cytoplasm	enzyme
CD47 molecule	Cd47	−0.417	0.00005	0.0131	Plasma Membrane	transmembrane receptor
cyclin-dependent kinase inhibitor 1C (P57)	Cdkn1c	0.408	0.00005	0.0131	Nucleus	other
centromere protein I	Cenpi	5.132	0.00005	0.0131	Nucleus	other
cholesterol 25-hydroxylase	Ch25h	−1.612	0.00005	0.0131	Cytoplasm	enzyme
coproporphyrinogen oxidase	Cpox	0.356	0.00005	0.0131	Cytoplasm	enzyme
RIKEN cDNA D430020J02 gene	D430020J02Rik	0.955	0.00005	0.0131	Other	other
dpy-19 like Cmannosyltransferase 1	Dpy19l1	0.394	0.00005	0.0131	Other	other
family with sequence similarity 107 member A	Fam107 a	−0.334	0.00005	0.0131	Nucleus	other
FAU ubiquitin like and ribosomal protein S30 fusion	Fau	1.474	0.00005	0.0131	Cytoplasm	other
FCH and mu domain containing endocytic adaptor 1	Fcho1	−0.44	0.00005	0.0131	Plasma Membrane	other
Fos proto-oncogene, AP-1 transcription factor subunit	Fos	−0.455	0.00005	0.0131	Nucleus	transcription regulator
FosB proto-oncogene, AP-1 transcription factor subunit glycerophosphodiester	Fosb	−0.913	0.00005	0.0131	Nucleus	transcription regulator
phosphodiesterase domain containing 3	Gdpd3	−1.986	0.00005	0.0131	Cytoplasm	enzyme
gap junction protein gamma 2	Gjc2	0.274	0.0001	0.0232	Plasma Membrane	transporter
G protein-coupled receptor 15	Gpr15	−0.753	0.00025	0.0483	Plasma Membrane	G-protein coupled receptor
gelsolin	Gsn	0.431	0.00005	0.0131	Extracellular Space	other
H2B clustered histone 11	H2bc21	−0.535	0.00015	0.0316	Nucleus	other
HemK methyltransferase family member 1	Hemk1	−0.711	0.00005	0.0131	Nucleus	enzyme
hypoxia inducible factor 3 subunit alpha	Hif3a	−0.641	0.00005	0.0131	Nucleus	transcription regulator

Entrez Gene Name	ID	Log_2(KO/WT)	P-value	FDR (q-value)	Location	Type(s)
3-hydroxy-3-methylglutaryl-CoA synthase 1	Hmgcs1	0.345	0.00005	0.0131	Cytoplasm	enzyme
homeobox A10	Hoxa10	−0.387	0.00005	0.0131	Other	transcription regulator
homeobox C10	Hoxc10	−0.356	0.00005	0.0131	Nucleus	transcription regulator
homeobox C8	Hoxc8	0.31	0.00005	0.0131	Nucleus	transcription regulator
homeobox D10	Hoxd10	−1.144	0.00005	0.0131	Nucleus	transcription regulator
heat shock protein family A (Hsp70) member 1A	Hspa1a	−0.954	0.00005	0.0131	Cytoplasm	enzyme
heat shock protein family A (Hsp70) member 1A	Hspa1b	−0.866	0.00005	0.0131	Cytoplasm	enzyme
heat shock protein family A (Hsp70) member 8	Hspa8	−1.216	0.00005	0.0131	Cytoplasm	enzyme
5-hydroxytryptamine receptor 3A	Htr3a	−0.697	0.0001	0.0232	Plasma Membrane	ion channel
intercellular adhesion molecule 1	Icam1	−1.407	0.00005	0.0131	Plasma Membrane	transmembrane receptor
kallikrein related peptidase 6	Klk6	0.266	0.00025	0.0483	Extracellular Space	peptidase
leucyl-tRNA synthetase 2, mitochondrial	Lars2	−0.346	0.00005	0.0131	Cytoplasm	enzyme
lipocalin 2	Lcn2	−1.557	0.00005	0.0131	Extracellular Space	transporter
lanosterol synthase	Lss	0.35	0.00005	0.0131	Cytoplasm	enzyme
lactotransferrin	Ltf	2.511	0.00005	0.0131	Extracellular Space	peptidase
major facilitator superfamily domain containing 2A	Mfsd2a	−0.321	0.00015	0.0316	Plasma Membrane	transporter
MOB kinase activator 3B	Mob3b	0.406	0.00005	0.0131	Other	other
metallothionein 2	Mt2	−0.34	0.00005	0.0131	Cytoplasm	other
neutrophilic granule protein	Ngp	2.851	0.00005	0.0131	Extracellular Space	other
neuropeptide S receptor 1	Npsr1	1.122	0.00005	0.0131	Plasma Membrane	G-protein coupled receptor
negative regulator of reactive oxygen species	Nrros	−0.712	0.0001	0.0232	Cytoplasm	other
neurexophilin and PC-esterase domain family member 4	Nxpe4	−0.574	0.00005	0.0131	Extracellular Space	other
prodynorphin	Pdyn	−0.582	0.00025	0.0483	Extracellular Space	transporter
phosphatidylserine decarboxylase, pseudogene 1	Pisd-ps1	−0.544	0.00005	0.0131	Other	other
phosphatidylserine decarboxylase, pseudogene 2	Pisd-ps2	−0.405	0.0001	0.0232	Other	other
POC1 centriolar protein A	Poc1a	0.941	0.00005	0.0131	Cytoplasm	peptidase
RAB7B, member RAS oncogene family	Rab7b	0.519	0.00005	0.0131	Cytoplasm	peptidase
REC8 meiotic recombination protein	Rec8	1.13	0.00005	0.0131	Nucleus	other
ribosomal protein L29	Rpl29	2.308	0.00005	0.0131	Cytoplasm	other

Entrez Gene Name	ID	Log_2(KO/WT)	P-value	FDR (q-value)	Location	Type(s)
ribosomal protein L34	Rpl34	−1.089	0.0001	0.0232	Cytoplasm	other
ribosomal protein L35a	Rpl35a	2.04	0.00005	0.0131	Cytoplasm	other
ribosomal protein L7	Rpl7	−0.327	0.00015	0.0316	Nucleus	transcription regulator
S100 calcium binding protein A8	S100a8	1.935	0.00005	0.0131	Cytoplasm	other
S100 calcium binding protein A9	S100a9	1.672	0.00005	0.0131	Cytoplasm	other
semaphorin 4D	Sema4d	0.277	0.00025	0.0483	Plasma Membrane	transmembrane receptor
serpin family A member 3	Serpina 3n	0.786	0.00005	0.0131	Extracellular Space	other
serum/glucocorticoid regulated kinase 1	Sgk1	−0.519	0.00005	0.0131	Cytoplasm	kinase
transferrin	Trf	0.327	0.00025	0.0483	Extracellular Space	transporter
transmembrane protein 117	Tmem117	0.339	0.00015	0.0316	Cytoplasm	other
transmembrane protein 35A	Tmem35a	−2.973	0.00005	0.0131	Other	other
trophoblast glycoprotein	Tpbg	−0.424	0.00005	0.0131	Plasma Membrane	other
tubulin alpha 1c	Tuba1c	1.727	0.00005	0.0131	Cytoplasm	other
UDP glycosyltransferase 8	Ugt8a	0.32	0.0001	0.0232	Cytoplasm	enzyme